

EXTRACELLULAR POTASSIUM ACCUMULATION IN VOLTAGE-CLAMPED FROG VENTRICULAR MUSCLE

BY LARS CLEEMANN AND MARTIN MORAD

*From the Department of Physiology, University of Pennsylvania,
Philadelphia, Pennsylvania 19104, U.S.A.*

(Received 8 May 1978)

SUMMARY

1. Application of voltage clamp pulses (1–10 sec) to frog ventricular strips causes temporary changes in the extracellular K concentration.

2. The changes in the extracellular K concentration can be estimated from (a) slowly decaying post-clamp after-potentials, (b) changes in the action potential duration, and (c) measurements with a K-selective micro-electrode.

3. The depolarization of the resting potential and the shortening of the action potential are present in approximately the same proportions during voltage-clamp induced extracellular K accumulation and during perfusion with a K-rich Ringer solution but small consistent differences are noticed.

4. The measurements of the after-potential, the action potential shortening, and the K-electrode response were analysed as indicators of extracellular K⁺ activity and it was concluded that the after-potential provides the most convenient and reliable estimate of the absolute magnitude of the voltage-clamp induced extracellular K accumulation.

5. The depolarizing after-potentials decay more slowly than the hyperpolarizing after-potentials but it is found that this reflects the selectivity of the membrane to K⁺ concentrations as predicted by the Nernst or the Goldman equations.

6. Analysis of the redistribution of accumulated K⁺ from the decay of the after-potential suggests that the major part of the redistribution process can be described by a single time constant (2–4 sec). A much longer time constant is required for a smaller component of the 'tail' in order to bring [K]_o to the normal resting state.

7. N-shaped relations similar to the 'steady state' current–voltage relation are obtained when the post-clamp after-potential, the action potential shortening, and the K-electrode response are plotted versus the clamped membrane potential. The maxima of these curves are located around –40 mV and the minima around –20 mV.

8. In spite of a significant outward membrane current (1–1.5 μA) in the minimum region (–20 mV), the post-clamp after-potential is often hyperpolarizing in nature suggesting extracellular K depletion.

9. These findings indicate that the K efflux is lower at –20 mV than at both higher and lower potentials and suggest that the N-shape 'steady state' current–voltage relation mainly reflects the voltage dependency of the K current.

10. A theory for K accumulation in a single compartment is presented which predicts that a simple linear RC-circuit may describe the electrical response of the

preparation in a limited potential range around the resting potential. The extracellular accumulation space was estimated to be 13–16% of the total volume of the preparation. It is tentatively suggested that the accumulation space is equivalent to the subendothelial fraction of the extracellular space.

INTRODUCTION

Experimental evidence from a number of excitable tissues indicates that a net K flux across the cell membrane may cause the K concentration just outside the cell membrane to be different from the concentration of K^+ in the bulk of the perfusing solution. This phenomenon is commonly known as extracellular K accumulation and is often attributed to the relatively slow equilibration of a restricted section of the extracellular space with the bathing solution. In the squid axon the extracellular K accumulation is thought to occur in the narrow space between the Schwann cells and the membrane of the axon. The limited exchange of this space is ascribed to diffusion through the narrow clefts between the Schwann cells (Frankenhaeuser & Hodgkin, 1956; Adelman, Palti & Senft, 1973). The K accumulation during a single action potential is of sufficient magnitude as to be of some importance during the late part of the repolarization and during the hyperpolarizing after-potential (Adelman & Fitzhugh, 1975).

The decay of the inward K current in hyperpolarized voltage-clamped fibres of frog sartorius muscle was shown not only to reflect slow deactivation of K^+ current, but also to be due to K depletion in the transverse tubular system (Adrian & Freygang, 1962; Almers, 1972*a, b*; Barry & Adrian, 1973).

Small transient changes in the extracellular K concentration were observed using K-selective micro-electrodes placed in the immediate vicinity of the exposed single neurones of the snail *Helix pomatia* (Neher & Lux, 1973). The observation that some K accumulation can occur even in an unrestricted extracellular space makes it reasonable to suspect much greater extracellular K accumulation in preparations where the extracellular ionic diffusion pathways are narrow and tortuous.

Unsuccessful attempts to measure unidirectional phasic fluxes in frog ventricular preparations have supplied the first indication that ions leaving the myocardial cells are retained in the preparation for some time before they appear in the perfusate (Lamb & McGuigan, 1968). On the basis of morphological studies it has been suggested that the endothelial sheath surrounding individual trabeculae may act as a barrier for ionic exchange between the subendothelial fraction of the extracellular space and the surrounding fluid (Page & Niedergerke, 1972). The calculated half-time for equilibration of Ca^{2+} through the narrow clefts of the endothelial sheath is comparable to the half-time for the fast inotropic Ca^{2+} response (Chapman & Niedergerke, 1970).

Niedergerke & Orkand (1966) found a depolarization of the resting potential when frog ventricular muscle was stimulated at a high frequency and related this to K accumulation in a confined space outside the membrane. Measurements with a K-selective micro-electrode have confirmed extracellular K accumulation under these conditions and have further shown that accumulation of about 1 mM- K^+ may be recorded during a single action potential (Kline & Morad, 1976). K^+ accumulation

has been also observed in other cardiac tissue: in Purkinje fibre (McAllister & Noble, 1966; Baumgarten & Isenberg, 1977), in sheep and calf ventricular muscle (McGuigan, 1974), and in frog atrial muscle (Noble, 1976).

In this report we present evidence for extracellular K accumulation in voltage-clamped frog ventricular muscle. The extracellular K accumulation has been estimated from after-potentials, changes in action potential duration and measurements with K-selective micro-electrodes. Potassium accumulation was measured as a function of the clamped membrane potential and the relationship was similar to the N-shaped steady state current-voltage relation suggesting that a major part of the maintained membrane current accompanying the clamp step is carried by K. Analysis of the kinetics of decay of accumulated K⁺ suggests that K⁺ accumulates primarily in a single compartment.

A preliminary report of these findings has been published (Cleemann & Morad, 1976).

METHODS

Quiescent strips 0.4–0.5 mm in diameter were dissected from the circular basal region of the ventricle of frogs (*Rana pipiens*). The strip was placed in the single sucrose gap and the membrane was voltage-clamped and the membrane current and tension were measured as described by Morad & Orkand (1971). The clamp loop could be closed and opened in synchrony with the beginning and the end of the clamp pulses using a fast electro-mechanical relay (delay 1–2 msec). This electronic procedure makes it possible to apply the clamp step without a previous holding potential and to detect the post-clamp membrane potential immediately after termination of the command pulse.

Solutions. The solutions normally perfused in the three compartments had the following composition (mM). (a) Ringer solution: NaCl 116; NaHCO₃ 2.0; KCl 3; CaCl₂ 0.2–1.0; (b) sucrose solution: sucrose 210 (special enzyme grade, Schwartz-Mann); MnSO₄ 0.01; (c) KCl Ringer: KCl 120; NaHCO₃ 2. All solutions were prepared with deionized and distilled water. In some experiments tetrodotoxin (TTX, Sigma) was added to the normal Ringer solution. In other experiments a Ringer solution with twice (6 mM) or half (1.5 mM) the normal K concentration was used. These solutions were prepared keeping the sum of the Na concentration and the K concentration constant.

Stimulation. The preparation was stimulated every 6 sec with pulses of 5 msec in width and approximately 5 μ A in amplitude. The stimulating current was passed between the KCl compartment and the Ringer compartment. Addition of TTX required stronger stimulating currents in order to elicit an action potential.

K electrode. In some experiments K-selective micro-electrodes were inserted into the preparation in order to measure directly the K activity in the extracellular space. The K electrode (Walker, 1971) was prepared by the technique described by Kline & Morad (1976, 1978). The tip diameter of the electrode was approximately 1–2 μ m with a selectivity of 60:1 for K:Na.

Tests and precautions. In addition to the precautions undertaken by Morad & Orkand (1971) and Goldman & Morad (1977a), the following rules were observed. A preparation was considered satisfactory only if the action potential at the end of the equilibration period had a duration of at least 300 msec and if intracellular recordings gave resting potentials more negative than –75 mV. The relatively small after-potentials caused by extracellular K accumulation could only be measured accurately if the intracellular micro-electrode recorded a stable resting potential from the normally stimulated preparation. A successful impalement of a cell with a micro-electrode was often followed for a couple of minutes by stabilization of the puncture which resulted in an increase in the resting potential and in the overshoot of the action potential. Occasionally continuous intracellular recordings for half an hour or more were obtained and the data used for illustrations, in all cases, has been obtained from such experiments. Records obtained from multiple impalements essentially produce similar results. Repetition of the same clamp pulses during an experiment lasting some hours gave membrane currents of slowly increasing magnitude. This increase has been related to an increase in the magnitude of the

leakage current across the sucrose gap (Goldman & Morad, 1977a). A sequence of clamp pulses was often finished by repeating the first clamp pulse. The increase in membrane current was barely measurable with a continuous puncture lasting half an hour. Sometimes a slow depolarization in order of a few mV was observed during continuous intracellular recording of the resting potential without any change of action potential (see Fig. 13). This effect was attributed to a change in the tip potential of the micro-electrode and the resting potential was appropriately corrected.

The operation of the ground clamp circuit was occasionally tested by passing long current pulses while the micro-electrode was placed in the Ringer compartment. Polarization of the voltage-sensing Ag/AgCl electrode might have produced an artifact resembling the after-potential but the flatness of the recorded potential trace indicated that the ground clamp loop supplied a low impedance pathway to ground for both high and low frequency currents.

Only preparations with small dimensions could be adequately voltage-clamped. The measured membrane current and isometric tension were essential for the screening of the records. The membrane current was required to be smooth during a clamp pulse, i.e. without any indication of 'notches' or 'upside-down' action potentials. In order to assure that only the part of the muscle in the Ringer contributed to the developed tension, the part of the strip in the sucrose pool was kept slack. The measured tension was required to be well-maintained during the clamp and without indication of a phasic component. The phasic tension which usually occurred simultaneously with the 'upside-down' current action potential was thought to represent poor clamp control of a part of the preparation.

The words 'membrane potential' and 'membrane current' are frequently used somewhat loosely. The preparations used in these experiments have a significant extracellular series resistance. Such a resistance causes a voltage drop that should be subtracted from the potential difference between the intracellular potential and the potential of the bathing solution in order to give the true transmembrane potential. The measured 'membrane current' included some leakage current which passed from the KCl compartment to the Ringer compartment without crossing the membrane of the myocardial cells in the Ringer compartment. The problem of the leakage current has been dealt with in detail elsewhere (Goldman & Morad, 1977a).

Theory

The relationship between the membrane current and the after-potential. The extracellular accumulation of K is described in terms of a model with three compartments: an intracellular compartment, a slowly exchangeable extracellular space, and the bathing solution. The three compartments are in series in such a way that ionic exchange between the bath and the intracellular compartment only can occur through the slowly exchangeable extracellular space. The ionic exchange between the intracellular compartment and the slowly exchangeable extracellular space is determined, in part, by the properties of the cell membrane; the exchange between the extracellular space and the bath is determined by the properties of a hypothetical 'second barrier'. The intracellular K concentration, K_i , and the K concentration of the bathing solution, K_o , are essentially constant due to the large K content of these two compartments, but the K concentration in the smaller slowly exchangeable extracellular space, K_e , is subject to fluctuations whenever there is an imbalance between the K fluxes across the cell membrane and across the second barrier. The K concentration in the slowly exchangeable extracellular space can only be described by a single value, K_e , if it is assumed that the various sections of the space either equilibrate rapidly with each other or receive a net K influx in proportion to their separate volumes. Let the volume of the extracellular accumulation space be V_e and let the outward K current across the cell membrane and the 'second barrier' be I_{mK} and I_{sK} respectively. The rate of K accumulation in the extracellular space is then given by the equation:

$$\frac{d}{dt} K_e = \frac{F}{V_e} (I_{mK} - I_{sK}), \quad (1.1)$$

where F is Faradays constant. The current across the cell membrane, I_m , can be separated in two parts, one which is carried by K^+ , I_{mK} , and one which is carried by other ions, I_{mr} (the residual current). Therefore:

$$I_m = I_{mK} + I_{mr}. \quad (1.2)$$

In the fully equilibrated preparation the K concentration in the extracellular space, K_e , can be assumed to be equal to the K concentration in the bathing solution, K_o . The accumulated K⁺ in the extracellular space, ΔK , caused by voltage clamp pulses is therefore:

$$\Delta K = K_e - K_o. \quad (1.3)$$

If P_{sK} is assumed to be the permeability of the second barrier to K then the loss of K from the accumulation space to the bath can be described by

$$I_{mK} = (K_e - K_o) \cdot \frac{P_{sK}}{F} = \Delta K \frac{P_{sK}}{F}. \quad (1.4)$$

Combination of eqns. (1.1), (1.2), (1.3) and (1.4) gives

$$\frac{d}{dt}(\Delta K) = \frac{1}{V_e} ((I_m - I_{mr})/F - \Delta K \cdot P_{sK}). \quad (1.5)$$

The time constant for this linear first order differential equation is

$$T_e = V_e/P_{sK}. \quad (1.6)$$

The K accumulation at time t_1 can be calculated as a convolution integral if I_m and I_{mr} are known as functions of time, t :

$$\Delta K = \frac{1}{F \cdot V_e} \int_0^{t_1} (I_m - I_{mr}) \cdot \exp\left(\frac{t-t_1}{T_e}\right) \cdot dt. \quad (1.7)$$

I_m is the measured membrane current, but the residual membrane current, I_{mr} , cannot be estimated without further assumptions. The K accumulation has been estimated from after-potentials measured in the absence of externally applied membrane current. A perfectly K-selective cell membrane would follow the Nernst equation for K, but it must be expected that other ions have some permeability. Using the constant field equation (Goldman, 1943) the relationship between the after-potential, ΔV , and the K accumulation, ΔK , takes the following form (McGuigan, 1974):

$$\Delta V = RT/F \cdot \ln \frac{\Delta K + K_o + K'_o}{K_o + K'_o}, \quad (1.8)$$

where R , T , and F have their usual values and K'_o is the extracellular K concentration which results in a unidirectional inward current equal to that carried by other ions.

The eqns. (1.7) and (1.8) link the after-potential, ΔV , to the membrane current, I_m . It is possible to obtain some information about T_e , K_o , V_e , and I_{mr} by comparing measured and calculated after-potentials. The equations have been used in this way in the following paper (Cleemann & Morad, 1978). In the present paper we have analysed the decay of the accumulated K⁺ and have estimated the size of the restricted extracellular space by application of small perturbations around the resting potential.

Linear approximation near the resting potential. This analysis will show that the extracellular K⁺ accumulation may cause a change in the K current, although the ionic conductances and permeabilities are constant. The discussion is limited to small voltage excursions from the resting potential so that linearity can be assumed. Around the resting potential, therefore, the ionic currents across the membrane into the restricted extracellular space can be described by the following equations:

$$I_{mK} = G_{mK} \cdot \Delta V_m - P_{mK} \cdot \Delta K \cdot F, \quad (1.9)$$

$$I_{mr} = G_{mr} \cdot \Delta V_m - P_{mr} \cdot \Delta K \cdot F. \quad (1.10)$$

The four transport coefficients, G_{mK} , G_{mr} , P_{mK} , and P_{mr} , completely describe the cell membrane in the linear region around the resting potential. The change in the potential difference between the intracellular compartment and the bathing solution, ΔV , is the change in the membrane potential, ΔV_m , plus the potential drop caused by series resistance, R_s :

$$\Delta V = \Delta V_m + I_m \cdot R_s. \quad (1.11)$$

The eqns. (1.2), (1.5), (1.9), (1.10), and (1.11) completely characterize the linear system. By substituting $j\omega$ for d/dt and eliminating I_{mK} , I_{mr} , and ΔV_m the following equations are obtained:

$$\Delta V = \left(\frac{1}{G_{mK} + G_{mr}} + R_s \right) I_m + \frac{P_{mK} + P_{mr}}{G_{mK} + G_{mr}} \cdot F \cdot \Delta K, \quad (1.12)$$

$$j\omega \Delta K \cdot V_e = \frac{G_{mK}}{G_{mK} + G_{mr}} \frac{I_m}{F} + \left(\frac{P_{mr} \cdot G_{mK} - P_{mK} \cdot G_{mr}}{G_{mK} + G_{mr}} - P_{sK} \right) \cdot \Delta K. \quad (1.13)$$

The electrical behaviour of the system can be given in closed form when ΔK is eliminated.

$$\Delta V = I_m \cdot \left[\frac{1}{G_{mK} + G_{mr}} + R_s + \frac{\frac{P_{mK} + P_{mr}}{G_{mK} + G_{mr}} \cdot \frac{G_{mK}}{G_{mK} + G_{mr}}}{j\omega V_e + \frac{P_{mK} \cdot G_{mr} - P_{mr} \cdot G_{mK}}{G_{mK} + G_{mr}} + P_{sK}} \right]. \quad (1.14)$$

This equation takes the simpler form:

$$\Delta V = I_m \cdot \left(R_m + R_s + \frac{R_e}{1 + j\omega R_e \cdot C_e} \right) \quad (1.15)$$

when the following parameters are introduced:

$$R_m = \frac{1}{G_{mK} + G_{mr}}, \quad (1.16)$$

$$R_e = \frac{\frac{P_{mK} + P_{mr}}{G_{mK} + G_{mr}} \cdot \frac{G_{mK}}{G_{mK} + G_{mr}}}{\frac{P_{mK} \cdot G_{mr} - P_{mr} \cdot G_{mK}}{G_{mK} \cdot G_{mr}} + P_{sK}}, \quad (1.17)$$

$$C_e = \frac{V_e}{\left(\frac{P_{mK} + P_{mr}}{G_{mK} + G_{mr}} \right) \left(\frac{G_{mK}}{G_{mK} + G_{mr}} \right)}. \quad (1.18)$$

Eqn. (1.15) corresponds to the simple RC circuit shown in Fig. 8 panel *C*. The resistance of the membrane, R_m , is not only in series with R_s but also with the parallel combination of a capacitor, C_e , and resistance, R_e . C_e , the accumulation capacitance, is proportional to the volume of the extracellular accumulation space, V_e , and depends on the properties of the cell membrane but it is independent of the permeability of the second barrier, P_{sK} , or the series resistance, R_s .

By linearizing eqn. (1.8) and by assuming that the membrane current, I_m , is zero in eqn. (1.12) the following relationship between the after-potential, ΔV , and the K accumulation, ΔK , is obtained:

$$\frac{\Delta V}{\Delta K} = \frac{RT}{F} \frac{1}{K_o + K'_o} = F \frac{P_{mK} + P_{mr}}{G_{mK} + G_{mr}}. \quad (1.19)$$

Combination of the eqns. (1.18) and (1.19) gives:

$$V_e = C_e \cdot \frac{G_{mK}}{G_{mK} + G_{mr}} \cdot \frac{RT}{F^2} \frac{1}{K_o + K'_o}. \quad (1.20)$$

This equation shows that the volume of the accumulation space can be determined from the accumulation capacity if it can be estimated to what extent the membrane current is carried by $K(G_{mK}/(G_{mK} + G_{mr}))$ and how accurately the membrane potential follows the equilibrium potential for $K(K'_o)$.

RESULTS

Fig. 1 illustrates the general experimental procedure used in this study. An original recording is shown in the top panel. The lower panel schematically shows that the records of the top panel are the result of measurements of membrane current, mem-

brane potential, and developed isometric tension during two consecutive sweeps. The stimulating current pulse, the normal action potential and the twitch tension are recorded during the first sweep. During the second sweep the membrane is clamped to -50 mV for 3.5 sec. Membrane current accompanying the clamp step is initially inward, changing rather rapidly to maintained outward current. The tension develops slowly during the beginning of the clamp and approaches a constant level towards the end of the clamp pulse. After the release of the voltage clamp, the current is zero, and the muscle begins to relax. The membrane potential first repolarizes rapidly, but

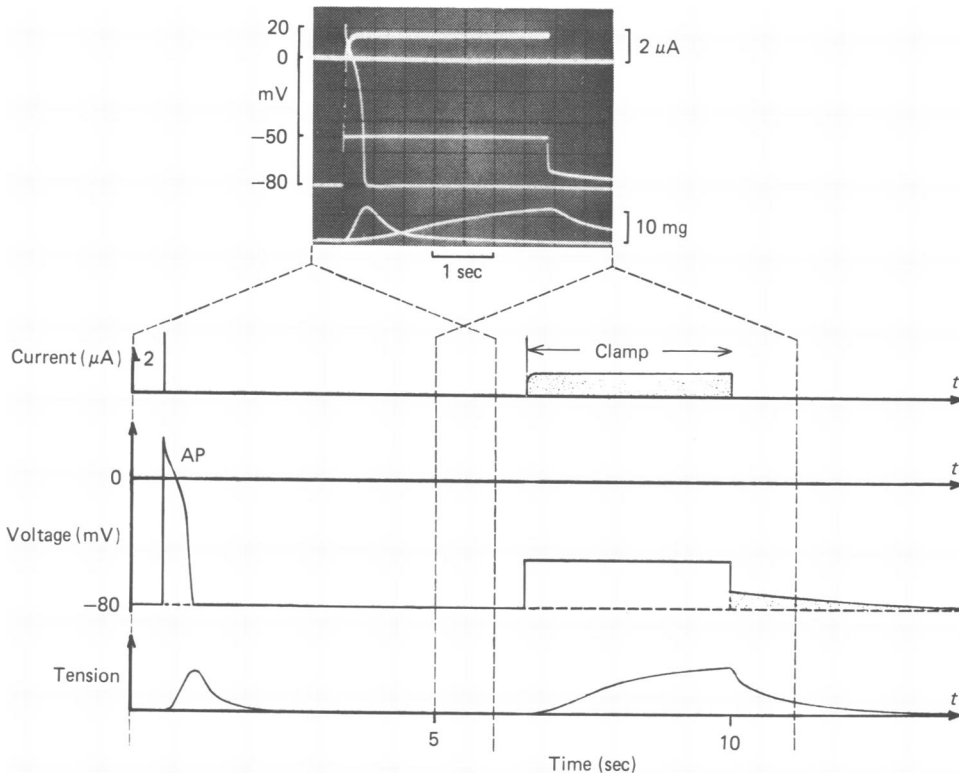


Fig. 1. Measurement of post-clamp after-potentials. The original record has superimposed traces from two consecutive sweeps. Membrane current, membrane potential (voltage) and isometric tension have been recorded. The two sweeps are diagrammatically shown below. The action potential and the associated stimulating current and twitch tension are recorded during the first sweep. During the second sweep the membrane potential is clamped to -50 mV for 3.5 sec. The upward deflexion of the current trace during the clamp pulse corresponds to outward (positive) membrane current. At the end of the clamp pulse the voltage clamp loop is opened, the membrane current is zero and a slowly decaying after-potential is observed.

the rapid repolarization is followed by a slowly decaying after-potential. With the slow time base used in these recordings the transition from the rapid fall to the slowly decaying after-potential appears as a sharp bend. The voltage difference between this bend and the normal resting potential is the quantity plotted in the experiments described below as the after-potential, ΔV .

The observation of the presence of post-clamp after-potential (Fig. 1) served as

the initial impetus to undertake this study. In the experiments to be described below an attempt is made to determine the time and potential dependence of the magnitude of the post-clamp after-potential, and to determine which ionic currents are responsible for it.

The effect of the clamped membrane potential on the K accumulation. Fig. 2 shows the after-potentials observed after release of clamp pulses to four different membrane potentials. The hyperpolarizing clamp pulse in panel A is followed by a hyperpolarizing after-potential. In the panels B and D the depolarizing clamp pulses are followed by depolarizing after-potentials, but in panel C, where the membrane is depolarized to -20 mV, there is no after-potential although there is a considerable

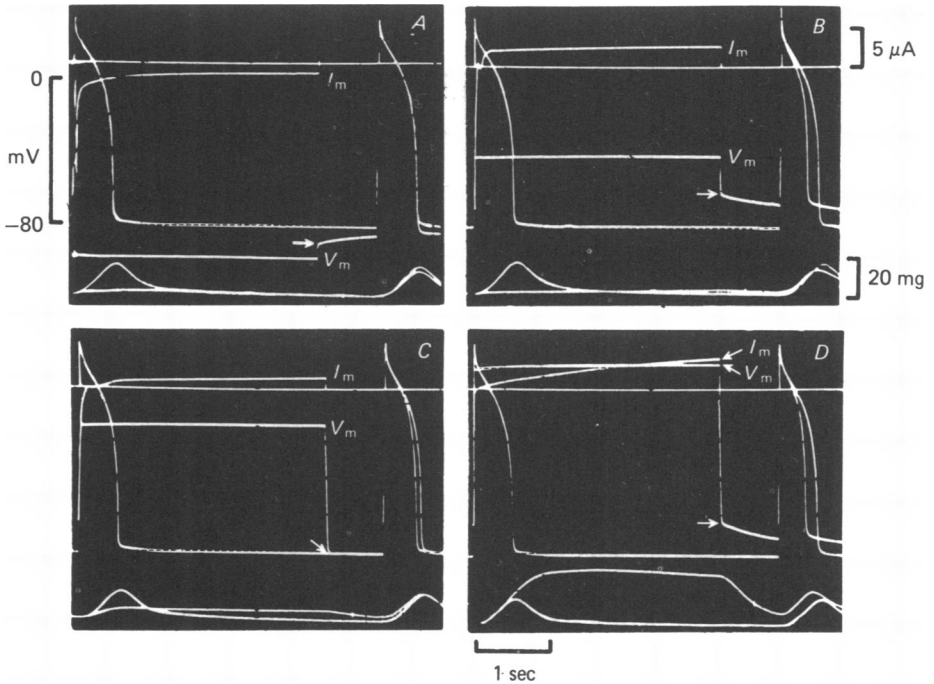


Fig. 2. The effect of the clamped membrane potential on the after-potential and the action potential duration. In each of the four panels the membrane potential (V_m), the membrane current (I_m) and the isometric tension are recorded as indicated in Fig. 1. The after-potentials are measured shortly after the release of the 3.4 sec clamp pulses (arrows). Test action potentials are stimulated 0.8 sec after the clamp pulses and are compared to normal action potentials. The change in the action potential duration is measured at a membrane potential of about -50 mV. The membrane current is measured at the end of the clamp pulses. The membrane potential is hyperpolarized in panel A and is depolarized in panels B, C, and D.

outward membrane current. In this experiment the action potential repetition cycle is adjusted such that an action potential occurs shortly after the termination of the clamp pulses at a time when the after-potentials still have a considerable magnitude. These action potentials are superimposed on normal action potentials and changes in the action potential duration can be clearly observed.

The measured values of membrane current, after-potential, and action potential

shortening are plotted in Fig. 3 versus the clamped membrane potential. The current-voltage relation has the characteristic N-shape with a minimum around -20 mV and a maximum around -40 mV. The after-potentials and the change in the duration of the post-clamp action potentials yield similar N-shaped relations when plotted versus the clamped membrane potential. The hyperpolarizing after-potentials are associated with a slight prolongation of the action potential. The results are consistent with clamp-induced changes in the extracellular K concentration, and suggest that the inward rectification of K^+ current may be responsible for the N-shaped current-voltage relation.

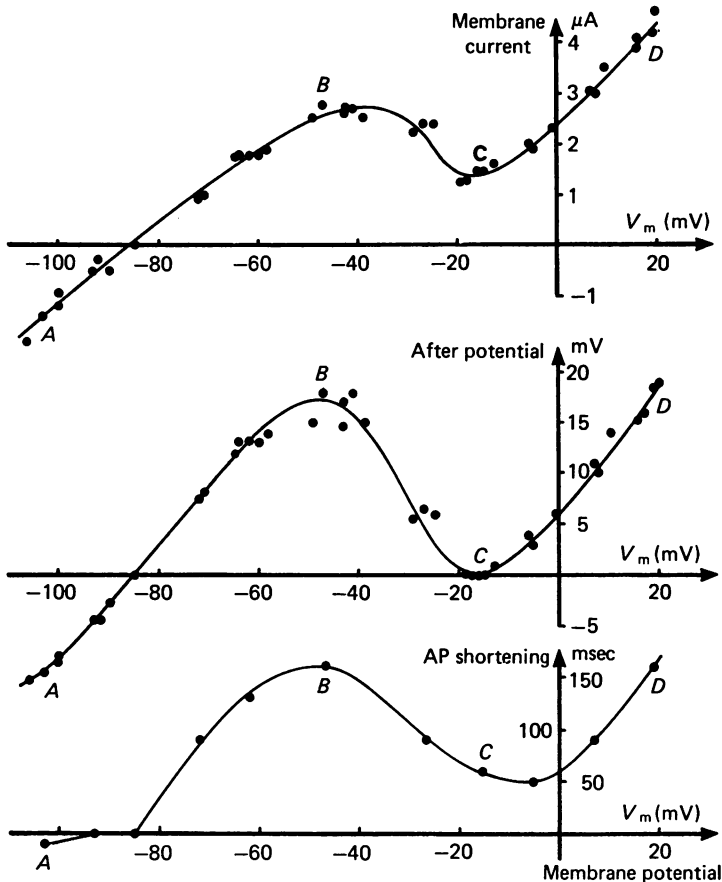


Fig. 3. The membrane current, the after-potential, and the action potential shortening versus the clamped membrane potential. The filled circles are obtained with clamp pulses of 3.4 sec duration. The points labelled A, B, C, and D correspond to the four panels in Fig. 2. Notice that the three plotted curves all are N-shaped and have maxima and minima around -40 and -20 mV respectively.

Direct evidence for extracellular K accumulation was obtained from experiments where K^+ -selective micro-electrodes were placed in an extracellular space in the ventricular strip. The lower panel of Fig. 4 shows the result from a 5 sec clamp pulse, accompanying membrane current, simultaneous recording from K^+ electrode, and an action potential which is stimulated 1.6 sec after the release of the clamp pulse.

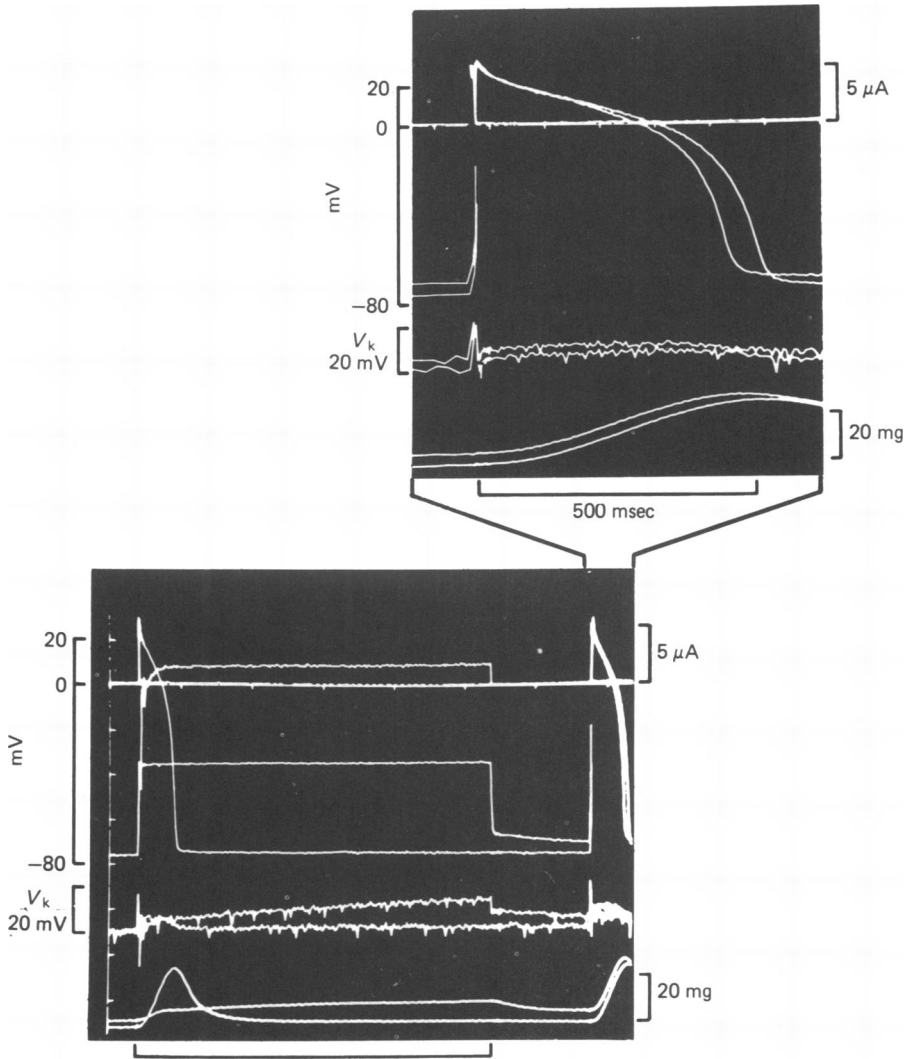


Fig. 4. Measurements with a single barrel K-selective micro-electrode. The records of membrane potential, membrane current, and isometric tension are supplemented with the trace from a K-selective electrode (V_k) placed in the extracellular space. The lower panel shows the records obtained during and after a 5 sec clamp pulse. A test action potential is stimulated 1.6 sec after the release of the clamp pulse. Duration of this action potential is compared to that of control in the upper panel. In the interval between the clamp pulse and the test action potential the K electrode records a potential similar to the slowly decaying after-potential. During the clamp pulse and during excitation the response of the K electrode is obscured by artifacts caused by the extracellular resistance. The experimental records were stored in digital form on magnetic tape and were replayed with different time base to produce the upper and the lower panel. In the upper panel the different appearance of the K electrode trace before and after the stimulation of the action potentials is due to different sampling rates.

This test action potential is displayed in the upper panel with expanded time-base and is compared to a normal action potential. With the K electrode placed in the muscle the measured potential is the sum of the potential caused by changes in the K activity and the electrical potential of the extracellular space. During the application of the voltage clamp step the flow of current through the series resistance adds a potential to the signal resulting from K accumulation. However, after the release

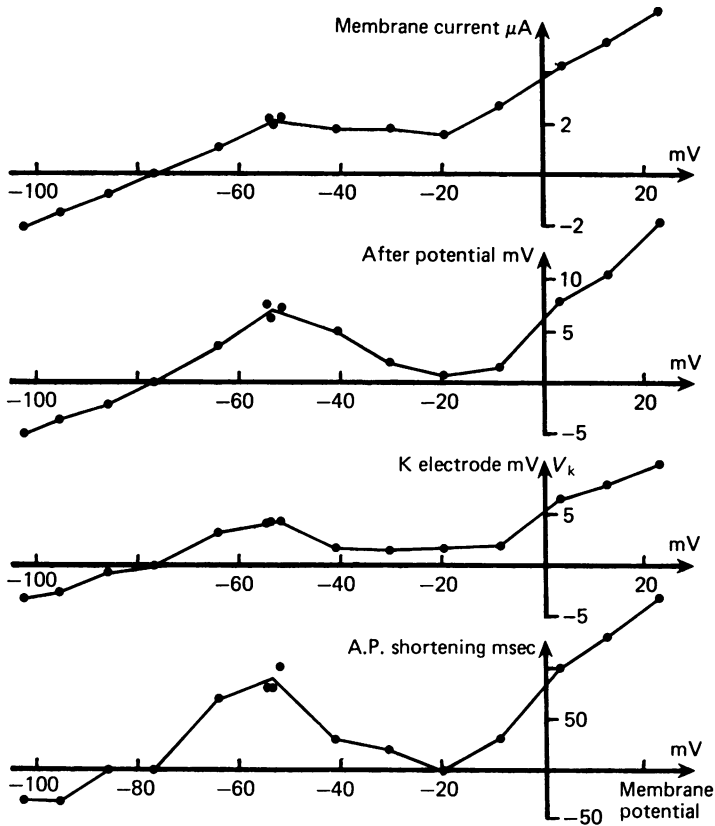


Fig. 5. Membrane current, after-potential, K electrode response, and action potential shortening versus the clamped membrane potential. As shown in Fig. 4 the duration of the clamp pulses was 5 sec and the test action potentials were stimulated 1.6 sec after the release of the voltage clamp step. The membrane current is measured at the end of the clamp pulse. The after-potential and the K electrode response were measured just before the test action potential. The three clamp pulses to potentials close to -55 mV were applied at the beginning, in the middle, and at the end of the sequence of clamp pulses to test the reproducibility. The four curves are similar and have maxima around -55 mV and minima around -20 mV.

of the clamp step, when there is no applied current, the K electrode measures mainly the K activity in the extracellular space and it records a slowly decaying potential similar to the after-potential recorded with the intracellular micro-electrode.

In Fig. 5 the membrane current at the end of the clamp pulse, the after-potential, the K electrode response and the action potential shortening were plotted versus the clamped membrane potential and all yield N-shaped relations. The similarity

of the three lower curves suggests that the after-potential, the K electrode response, and the action potential shortening can be used as indicators of extracellular K accumulation. These three parameters indicate that the K accumulation is functionally related to the membrane potential in almost the same way as is the membrane current. It is therefore reasonable to assume that a major part of the maintained membrane current is carried by K ions.

Comparison of net membrane current and ΔV potential around -20 mV in Fig. 5 reveals that although there is little or no indication of K^+ accumulation there is significant outward current at these clamped potentials. In some experiments careful

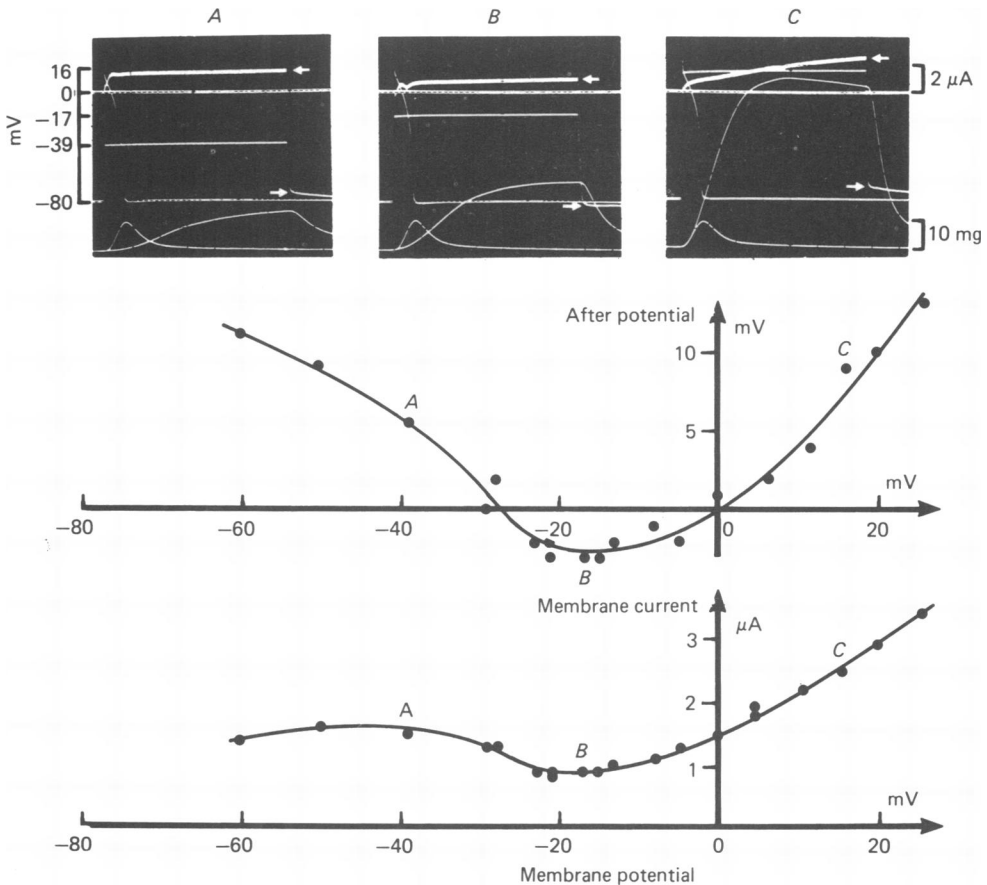


Fig. 6. Hyperpolarizing after-potentials produced by depolarizing clamp pulses to potentials around -20 mV. The after-potential and the membrane current are plotted versus the clamped membrane potential. The inset panels *A*, *B*, and *C* show samples of experimental records. The plotted values are indicated with arrows. A hyperpolarizing after-potential is clearly visible in panel *B*. Hyperpolarizing after-potentials are measured in the potential range from -25 to 0 mV.

examination of the minimum region shows 3–5 mV hyperpolarizing after-potentials, despite the presence of outward current (Fig. 6). The usual N-shape relation with a hyperpolarizing after-potential around 20 mV is observed when the after-potential is plotted versus the clamped membrane potential. The hyperpolarizing after-

potentials reach their maximum value with the clamp pulses of 1–2 sec duration. An action potential stimulated during a hyperpolarizing after-potential, following a clamp pulse to -20 mV, did not in general show prolongation as would be expected if the action potential duration was only controlled by the activity of K in the extracellular space. In this context it was noted that there was often a relatively small prolongation of the action potential during the more prominent hyperpolarizing after-potentials which follow hyperpolarizing clamp pulses (see Fig. 3).

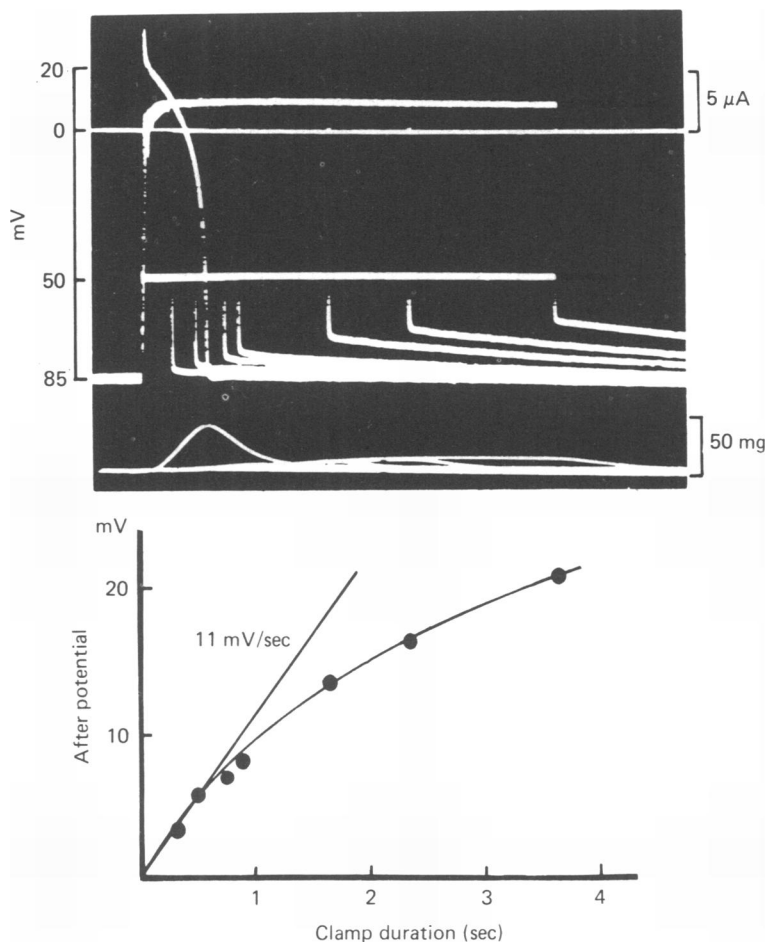


Fig. 7. Rate of development of the after-potential. The development of the after-potential is studied by clamping the membrane potential to -50 mV for various durations. The after-potentials are measured from the records in the upper panel shortly after the release of the voltage clamps and are plotted in the graph in the lower panel with the same time scale but with an expanded ordinate. The current traces and the tension traces recorded with the different clamp pulses superimpose well as long as the voltage clamp is maintained thereby indicating good reproducibility.

In the experiments described thus far we have studied only the magnitude of the extracellular K accumulation with respect to the membrane potential. The results indicate that a major part of the membrane current, but not all of it, appears to be

related to the K accumulation. In the following section we will describe the kinetics of the accumulation process in order to be able to separate the K current from the measured net membrane current.

Development of the after-potential. Fig. 7 illustrates an experiment where the membrane potential was clamped to -50 mV for various durations. The top panel shows the original records. In the bottom panel the after-potential measured shortly after release of the clamp pulse, is plotted versus the clamp duration. The magnitude of the after-potential increases continuously with increasing clamp duration while the membrane current remains fairly constant after the first 200 msec. The after-potential

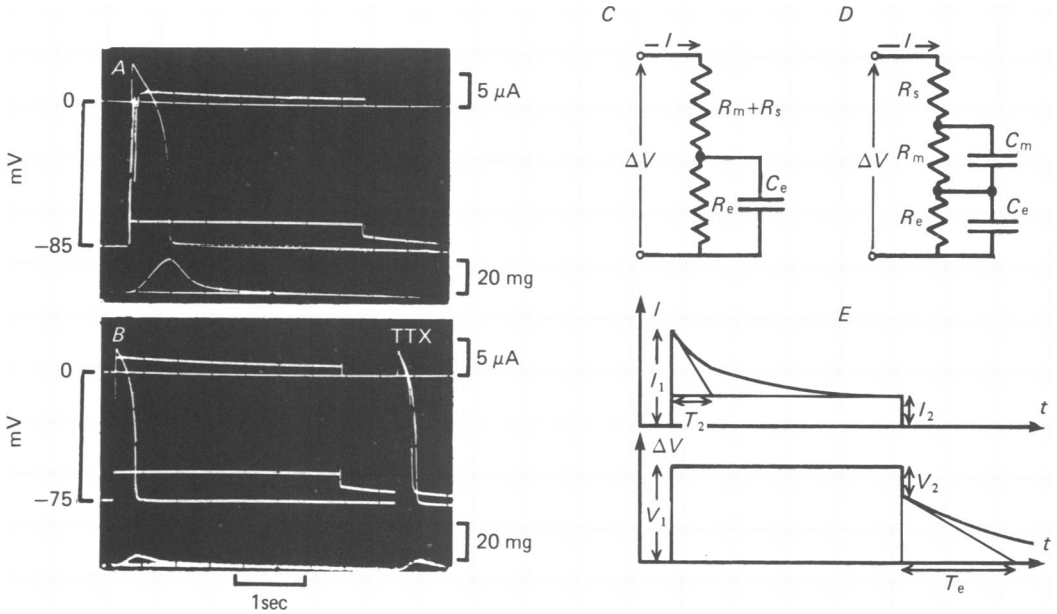


Fig. 8. Linear analysis in the potential region around the resting potential. Panels *A* and *B* show experimental records where the membrane is clamped to a slightly depolarized potential. The rapid inward current spikes seen in panel *A* are blocked by addition of 10^{-6} M-TTX (panel *B*). The voltage clamp records in panels *A* and *B* have been analysed as shown in panel *E*. The curves in panel *E* are predicted from the equivalent circuit in panel *C*. R_m and R_e are the membrane resistance and extracellular series resistance respectively. The electrical manifestations of extracellular K accumulation is related to the circuit elements R_e and C_e . The equivalent circuit in panel *D* shows the membrane capacitance, C_m , in parallel with the membrane resistance, R_m , and indicates that R_e and R_m may be separated by measuring the high frequency response of the preparation.

develops initially at a rate of approximately 11 mV/sec but the rate declines markedly when the clamp duration exceeds 1 sec. Two factors may contribute to this decline: (1) the logarithmic relationship between the extracellular K concentration and the resting membrane potential; and (2) the increase in the K concentration may increase the K efflux from the extracellular space. In the experiment illustrated in Fig. 7 the membrane current is approximately $2.3 \mu\text{A}$. A rough estimate indicates that this current, if carried entirely by K, is sufficient to depolarize the membrane and produce the measured after-potential shown in Fig. 7. In 1 sec a K current of $2.3 \mu\text{A}$

will carry 2.3×10^{-6} C or 2.3×10^{-11} M across the membrane. The preparation is about 0.5 mm long and has a diameter of about 0.45 mm. The estimated volume of the preparation is therefore $0.5 \text{ mm} \times (0.45 \text{ mm})^2 \times (\frac{1}{4}\pi) \times 10^{-6} \text{ l./mm}^3 = 8.7 \times 10^{-8} \text{ l.}$ The volume of subendothelial fraction of the extracellular space is about 10% of the preparation (Page & Niedergerke, 1972). Thus addition of 2.3×10^{-11} M-K⁺ to this space (0.8×10^{-8} l.) will increase the K concentration by $(2.3 \times 10^{-11} \text{ M}) / (0.8 \times 10^{-8} \text{ l.}) = 2.64 \text{ mM.}$ That is, the final concentration of K⁺ in the subendothelial fraction will be $3 + 2.64 \text{ mM} = 5.64 \text{ mM.}$ The change in the resting potential calculated from the Nernst equation is $25.4 \text{ mV} \times \ln(5.64/3) = 16 \text{ mV.}$ This is in reasonable agreement with the measured 11 mV of depolarization when considering that the membrane neither during nor after the clamp pulse can be expected to be perfectly K⁺ selective.

Linear approximation near the resting potential. The description of accumulation process and of the membrane properties in the potential region around the resting potential (-100 to -60 mV) is of special interest primarily for two reasons: (1) the after-potential is usually in the range of resting potential no matter what the magnitude of the clamp pulse that generates it, and (2) the predictions of linear theory with respect to the experimental results can be tested. Fig. 8C represents the electrical equivalent circuit derived in the theory section. This circuit responds to a voltage clamp step (V_1) as shown in Fig. 8E. The membrane current decays exponentially with the time constant T_2 from the initial value I_1 and approaches a steady value, I_2 , at the end of a long clamp pulse. After the clamp pulse the membrane depolarizes rapidly by the amount V_2 and then approaches the resting potential exponentially with the time constant T_e . These six quantities are related to the circuit elements by the eqns. (1.21), (1.22), and (1.23):

$$x = \frac{R_m + R_s}{R_m + R_s + R_e} = \frac{V_2}{V_1} = \frac{I_2}{I_1} = \frac{T_2}{T_e}, \quad (1.21)$$

$$R_m + R_s = V_1/I_1, \quad (1.22)$$

$$R_e \cdot T_e = C_e. \quad (1.23)$$

The records in Fig. 8A and B resemble the theoretical curves obtained in Fig. 8E. The fast inward-going current spikes of Fig. 8A are only observed when the membrane is depolarized more than approximately 10 mV and they disappear on addition of 10^{-6} M-TTX (Fig. 8B). This fast inward current is most likely related to the excitatory Na current and it has been disregarded in the present analysis.

Fig. 9 shows experimental data obtained by analysing a number of voltage clamp records according to Fig. 8E and eqns. (1.21), (1.22), and (1.23). The values measured in the presence of 10^{-6} M-TTX (filled circles) are not significantly different from the values obtained in the absence of TTX (open circles). The vertical bars indicate the accuracy of the plotted values calculated from a measurement accuracy, estimated to be 0.5 mV, $0.1 \mu\text{A}$, and 0.25 sec for potentials, currents and time constants, respectively. Within the accuracy of the measurements the plotted points can be approximated by straight lines. Had the system been perfectly linear the lines would be horizontal. The small signal parameters have been determined from the intercepts between the ordinates and the sloping lines. The five values obtained from the graphs give more than sufficient information to determine the three elements of the equivalent circuit ($R_m + R_s$, C_e , R_e). The horizontal dashed line connecting

the three lower graphs of Fig. 9 indicates that the measurements of potentials, currents, and time constants give approximately the same signal estimates for the impedance ratio (x) (eqn. 1.21).

In Fig. 9 the time constant values (T_e and T_2) are determined graphically. This method is neither very accurate nor does it test if it is permissible to use a small signal equivalent circuit with a single time constant. To overcome these shortcomings a minicomputer (Alpha 16, Computer Automation, Inc.) was used to perform a rigorous analysis of the voltage clamp results as shown in Fig. 10. The traces associ-

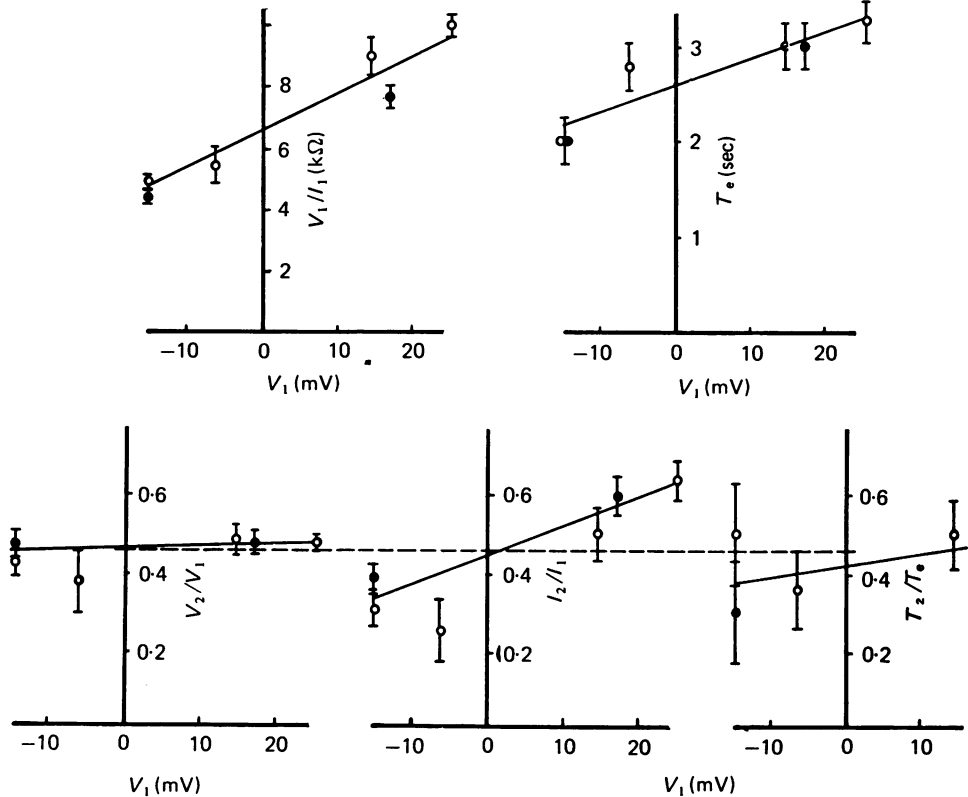


Fig. 9. Estimation of small signal parameters. Voltage clamp records have been analysed graphically using the method shown in Fig. 8 panel *E* and the results are plotted versus the amplitude of the clamp pulse. Open circles and filled circles correspond to measurements before and after the addition of 10^{-6} M-TTX. The measured points are approximated by sloping curves. The intersects between these curves and the ordinate axis give the small signal values listed in Table 1 as preparation no. 2. The dashed line connecting the three lower graphs confirm that the impedance ratio, x , may be estimated from three independent measurements as indicated by eqn. (1.21). The slope of the curves indicate deviations from linearity.

ated with individual voltage clamp pulses could well be approximated by curves of the form predicted from the equivalent circuit. The six parameters were determined using a least-squares method. Only the first 5 sec of the after-potentials were subjected to analysis. The single exponentials seem quite sufficient to describe the slow changes in membrane current and membrane potential. The upper right-hand graph of Fig. 10 shows that the small signal value for the impedance ratio, x , has about the

same value whether it is determined from the potential, current, or the time constant ratios. The small signal parameters from a number of experiments are listed in Table 1. The average value and standard deviation of the elements of the equivalent circuit are $R_m + R_s = 7.6 \pm 2.3$ K, $R_e = 10.4 \pm 3.4$ K, $C_e = 260 \pm 80$ μ F.

To determine the membrane resistance, in a number of experiments the extra-cellular series resistance was measured by the method described previously (Goldman & Morad, 1977a and Fig. 8D). Values obtained from such measurements are listed in Table 1 and have been subtracted from the value $R_s + R_m$ to give an estimate of the membrane resistance: $R_m = 4.5 \pm 1.4$ k Ω (S.D.).

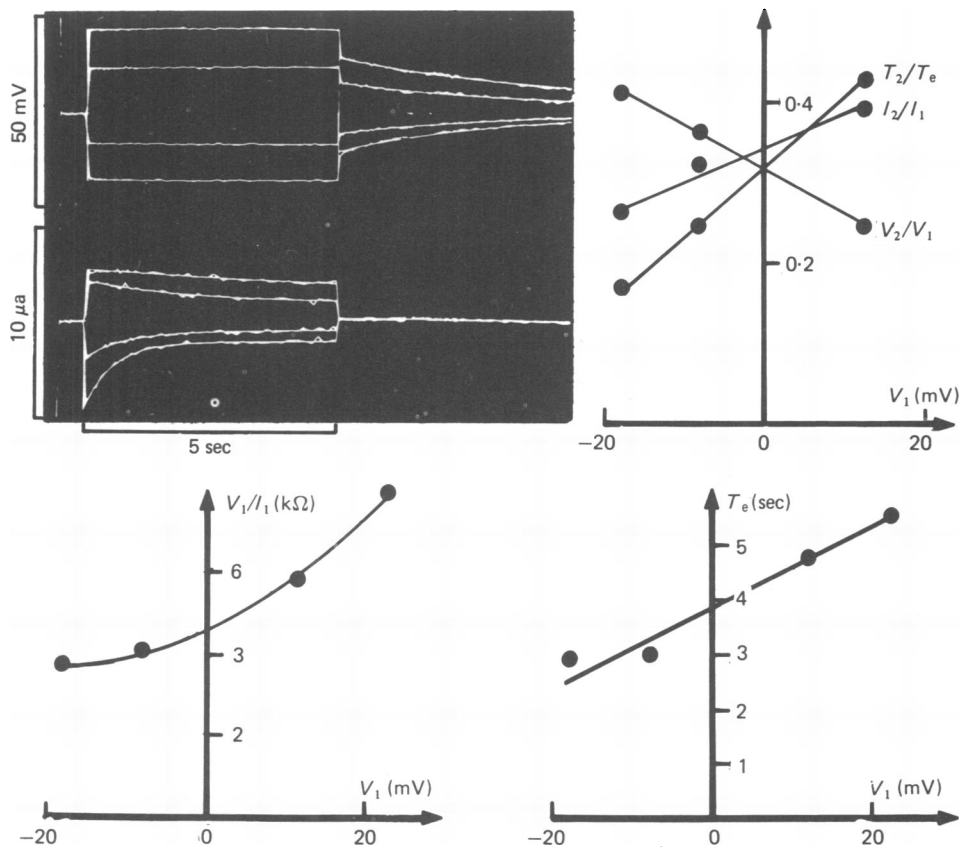


Fig. 10. Computer stimulation of the time course of the membrane potential and membrane current recorded during four clamp pulses. The quantities V_1 , V_2 , I_1 , I_2 , T_1 and T_2 (see Fig. 8 panel E) are determined using numerical analysis. The small signal parameters corresponding to the eqns. (1.21), (1.22), and (1.23) are estimated by plotting the measured values versus the amplitude of the clamp pulse, V_1 . The results are listed in Table 1 as preparation no. 4 (10^{-6} M-TTX).

The slope of the curves in Figs. 9 and 10 indicates that less than 5 mV voltage excursion from the resting potential can be tolerated before the deviation from linearity exceeds 10%. Contributing to this non-linearity is the inward-going rectification which is indicated by the observation that the resistance (V_1/I_1) is smaller for hyperpolarizing than for depolarizing clamp pulses (see Figs. 9 and 10).

TABLE 1. The components of the linear small signal equivalent circuit. The elements of the equivalent circuits in Fig. 8 panels *C* and *D* are estimated for seven experiments without (-) and with (+) 10^{-6} M-TTX and average values and standard deviations (s.d.) are calculated. The three first columns with numbers list values estimated as shown in Figs. 9 and 10. In the next two columns R_s and C_s are calculated using first eqn. (1.21) and then eqn. (1.23). The series resistance, R_s , is estimated from the fast potential jump in response to the stimulating current pulse. The membrane resistance, R_m , is obtained by subtracting the series resistance, R_s , from the total measured resistance, $R_m + R_s$. With depolarization of about 30 mV the initial membrane current, I_1 , reaches a maximum value which is listed as $I_{K, \max}$ and is multiplied by R_m to give an index for the degree of inward-going rectification. Measurements of the membrane capacitance, C_m , in preparations with similar dimension and membrane resistance give values about $1 \mu\text{F}$ (Goldman & Morad, 1977b).

Preparation no.	TTX, 10^{-6} M	$X = \frac{V_2}{V_1} = \frac{I_2 T_2}{I_1 T_1}$	$\frac{R_m + R_s}{V_1} \frac{I_1}{I_2}$ (k Ω)	T_s (sec)	$\frac{R_s}{1-x}$ (k Ω)	$C_s = T_s/R_s$ (μF)	R_s (k Ω)	R_m (k Ω)	$I_{K, \max}$ (μA)	$R_m \cdot I_{K, \max}$ (mV)
1	-	0.39	6.5	2.8	10.2	270	3.0	3.5	2.3	8.0
2	-/+	0.46	6.6	2.6	7.8	330	2.8	3.8	2.4	9.0
3	-	0.43	7.4	2.4	9.8	240	3.8	3.6	2.4	8.5
4	+	0.32	4.7	3.8	10.0	380			2.6	
5	+	0.53	10.8	2.0	9.6	210	5.5	5.3	1.9	10.0
6	-	0.38	10.8	2.5	17.6	140	3.8	7.0	1.5	10.5
7	-	0.50	7.5	2.0	7.5	270	3.5	4.0	1.9	7.5
Average		0.43	7.8	2.6	10.4	260	3.7	4.5	2.1	8.9
S.D.		0.07	2.2	0.6	3.4	± 80	1.0	1.4	± 0.4	± 1.2

An index for the degree of inward-going rectification has been obtained by measuring the maximal value for the initial membrane current, $I_{K, \max.}$ and multiplying by the membrane resistance, R_m . The results are listed in Table 1 and are remarkably constant from preparation to preparation: $R_m \cdot I_{K, \max.} = 8.9 \pm 1.2$ mV (s.d.). The significance of this value is discussed in the following paper where the inward-going rectification is treated more extensively. Another indication of non-linear behaviour is that the time constant for the decay of the after-potential depends on the magnitude of the clamp pulse (see Figs. 9 and 10). This is the second non-linearity to be treated quantitatively below.

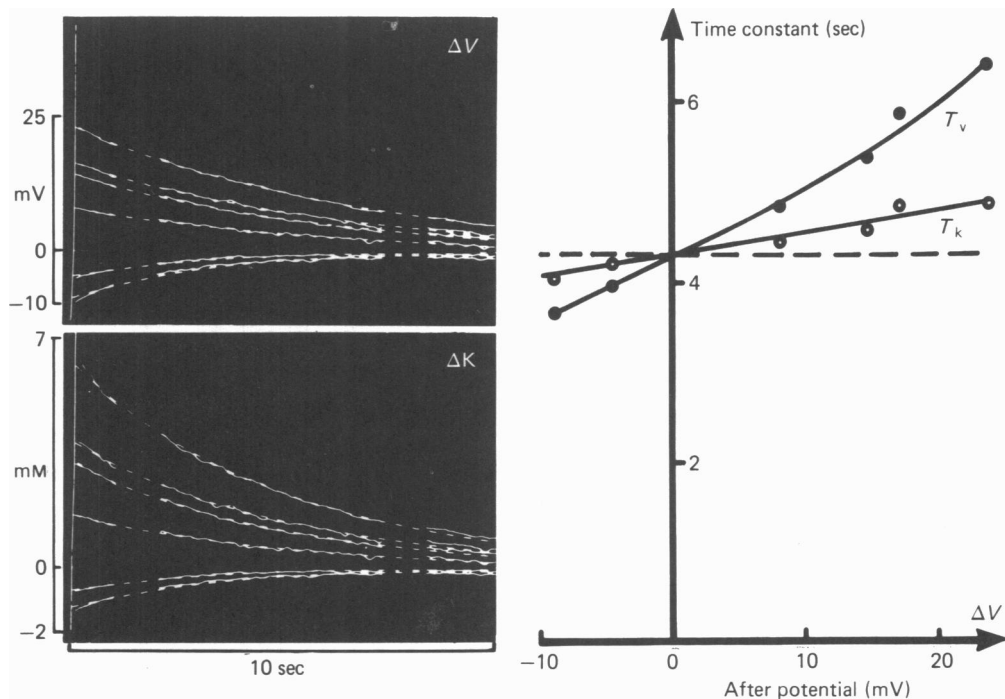


Fig. 11. The decay of the after-potential and of the accumulated K. In panel ΔV measured after-potentials are approximated by single exponentials. The time course of the redistribution of the accumulated K is examined in the same way in panel ΔK . The K accumulation is estimated from the after-potential using equation (1.8) with $K_o = 3$ mM and $K'_o = 1$ mM. The graph shows that the time constant for the redistribution of accumulated K depends much less on the initial magnitude of the after-potential than does the time constant for the after-potential (10^{-6} M-TTX).

The decay of the after-potential. The study of the decay of the after-potentials provides information on the redistribution of accumulated K. It was consistently noticed that small depolarizing clamp pulses give rise to after-potentials which decay more slowly than the after-potentials which follow slightly hyperpolarizing clamp pulses. Analysis of the after-potentials resulting from clamp pulses ranging from -100 to $+30$ mV suggests that variations in the time constant for the decay of the after-potential are more closely related to the initial magnitude of the after-potential than to the magnitude of the clamped membrane potential (Fig. 11). The time course of a number of post-clamp after-potentials is shown in the panel labelled ΔV . Each

after-potential has been approximated by a simple exponential with an initial amplitude and a time constant which are adjusted by numerical analysis to give the best fit for the 10 sec interval. The exponentials are plotted as dashed curves (panel ΔV) which can be seen distinctly in the gaps left open by the graphic removal of the action potential. Note that the theoretical approximations can hardly be distinguished from the measured curves. The curve labelled T_V is the time constant of the decay process plotted as a function of the amplitude of the after-potential. In the panel labelled ΔK the after-potentials are converted, point by point, to changes

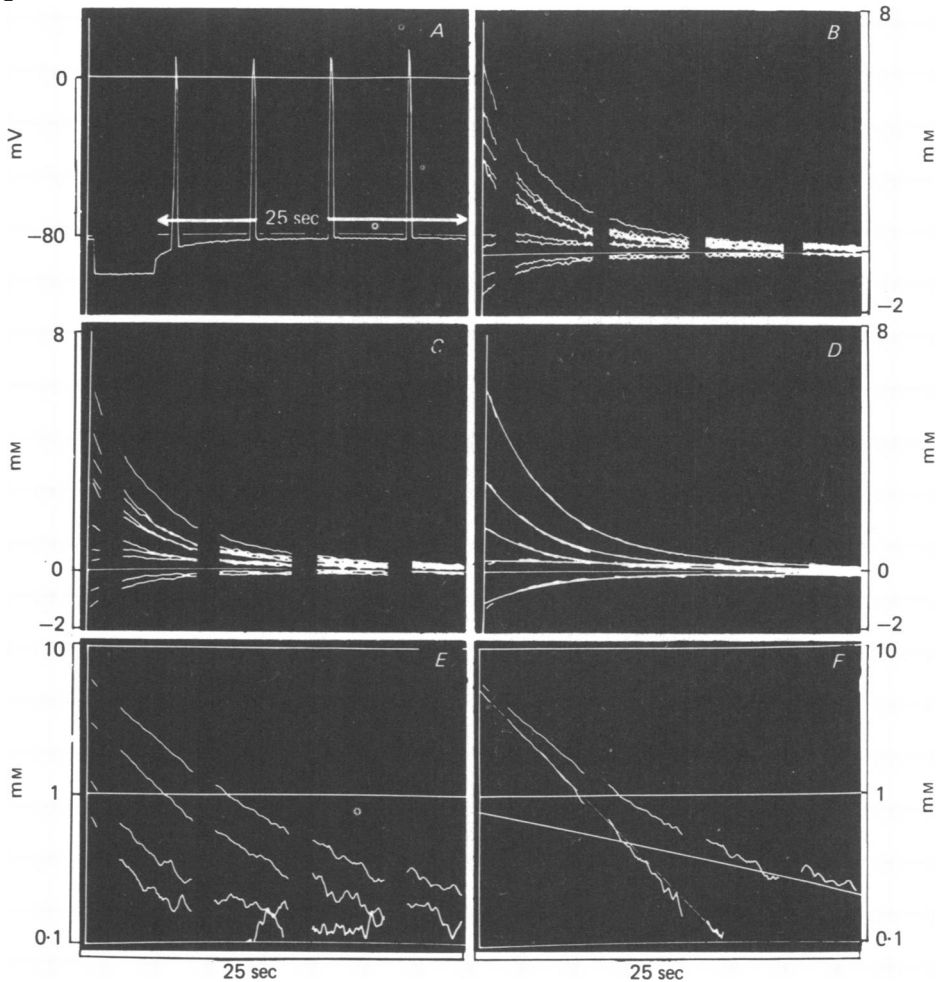


Fig. 12. Analysis of the redistribution of accumulated K using two time constants. After-potentials measured for 25 sec after the clamp pulses (panel A) are converted to change in the extracellular K concentration (panel B) using eqn. (1.8), with $K_0 = 3$ mM, and $K'_0 = 1$ mM. The records are filtered (panel C) and are approximated with curves which are the sum of two exponential functions (panel D). The two time constants (18.5 sec and 4 sec) are determined from the semilogarithmic plots (panels E and F). The two lower traces in panel E represent K depletion and the two upper traces, K^+ accumulation. In panel F the two time constants are determined from upper curves in panel E. The slowest exponential (18.5 sec) is determined by a straight line fitted to the late part of the curve and has been subtracted from the measured value in order to determine the fast exponential (4 sec).

in the extracellular K concentration using eqn. (1.8). The curves for the estimated K accumulation, or depletion, have been approximated by single exponentials. The time constants (T_K) are plotted in the graph (open circles) and is less potential dependent than T_V . This finding suggests that the accumulated K is redistributed with a time constant which is almost independent of the amount of accumulation.

More rigorous analysis of decay of post-clamp after-potentials of Fig. 11 reveals that it is a simplification to describe the K redistribution process by a single exponential. The analysis in Fig. 12 was performed to quantify the deviation from the single exponential decay. Panel *A* shows the results from a preparation where the after-potential was measured in the first 25 sec following 5 sec clamp pulses. Figs. 12*B-F* are based on after-potentials measured in the 25 sec interval following the release of the clamp pulses. The action potentials stimulated 1, 7.5, 14, and 20.5 sec after the end of the clamp have been omitted. Selected after-potentials were converted to changes in the extracellular K concentration using eqn. (1.8) and are plotted in panel *B*. Each point plotted in panel *C* is the average of five points plotted with 125 msec intervals in panel *B*. In panel *D* the records from panel *C* have been approximated by curves which are the sum of two exponential functions. The time constants for the two exponentials have been determined as indicated in panels *E* and *F*, where the logarithm of the absolute value of the K accumulation has been plotted. Once the time constants 18.5 and 4 sec were determined it was possible to assess the relative contribution of the two exponentials to the different after-potentials. It was found that the initial magnitude of the slowly decaying exponential with most clamp pulses was approximately one eighth of the initial magnitude of the more rapidly decaying exponential.

A further understanding of the K^+ redistribution process may also be gained by comparing the decay of after-potentials to the recovery of the action potential duration and to the decay of the K activity in the extracellular space. The action potentials, omitted from the traces of Fig. 12, are plotted with expanded time base in Fig. 13. Panels *A*, *B*, *C*, and *D*, show action potentials recorded during the decay of post-clamp after-potentials from clamps of -100 , -50 , -20 , and $+15$ mV, respectively. Each panel shows four action potentials which were stimulated at 1, 7.5, 14, and 20.5 sec after the release of the voltage clamp pulse. Each action potential was subjected to computer analysis and was approximated by a number of straight lines. Intersecting straight lines were used to approximate the resting potential, the upstroke, the plateau, and the rapid repolarization phase of the action potential. The duration of the action potential is measured as the time from the beginning of the stimulus to the point where the line representing the phase of rapid repolarization intersects the resting potential. The analysis shows that of the five parameters used to describe the action potential only the duration of the action potential and the resting potential seem to change significantly during the time course of the decay of the after-potential. The values measured from each of the four panels in Fig. 13 are represented by a curve which indicates how the membrane potential and the action potential duration return simultaneously to the control values after the release of the voltage clamp pulse. The deviation of the four curves (labelled *A*, *B*, *C*, and *D*) from a continuous single line may be in part due to a slow drift in resting potential (-83 to -80 mV) and action potential duration (350–290 msec).

The K accumulation measured using the K-sensitive micro-electrode does not follow the decay of the after-potential closely. It can be observed in Fig. 4 that the after-potential in the first second after the release of the clamp pulse falls more rapidly than the K electrode response.

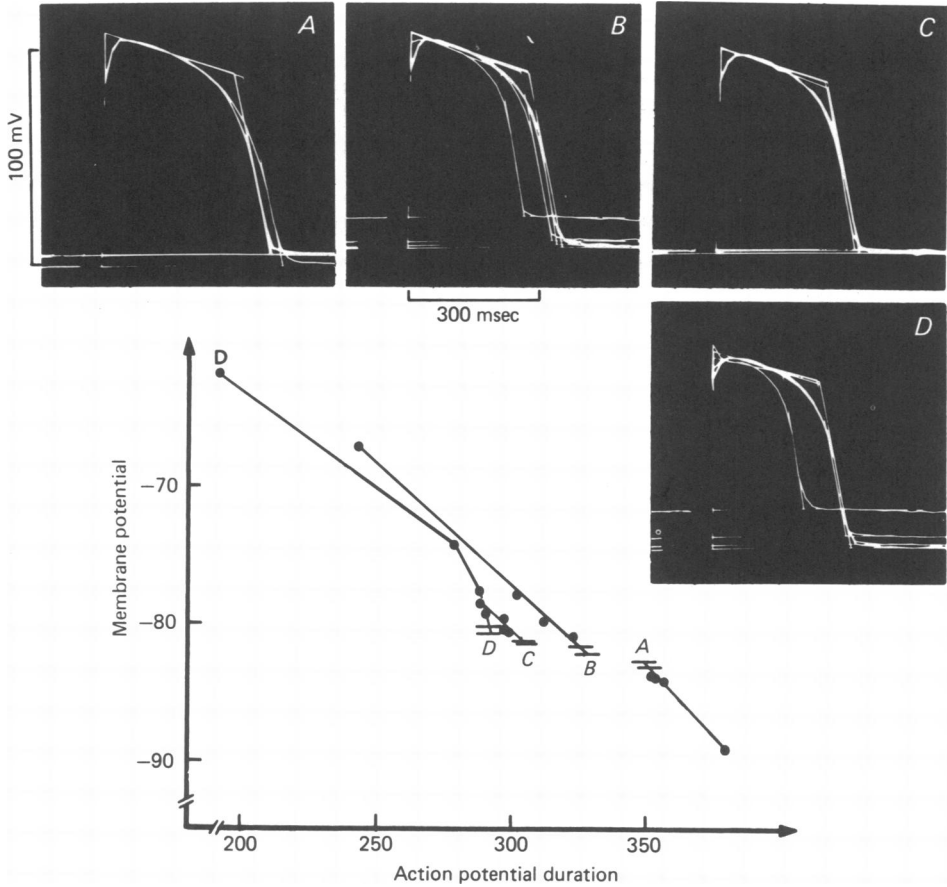


Fig. 13. Changes in the shape of the action potential measured during after-potentials. Each inset panel shows action potentials stimulated 1, 7.5, 14, and 20.5 sec after the release of the voltage clamp pulse. Each of the action potentials is approximated by four straight lines representing the resting potential (horizontal), the upstroke (vertical), the phase of slow repolarization and the phase of rapid repolarization. The computerized analysis shows that the rates of slow and rapid repolarization and the intersect between the lines representing the upstroke and the slow repolarization do not change significantly. The graph compares the changes in the two remaining independently determined quantities: the resting potential and the action potential duration. The four curves correspond to the four inset panels. The horizontal bars close to the labels indicate the resting potential measured before the clamp pulse and a couple of minutes later before the next clamp pulse. (10^{-6} M-TTX).

Changes in action potential duration caused by post-clamp K accumulation and variations in $[K]_o$. To quantify the post-clamp K accumulation, we have examined the effect of $[K]_o$ on resting and action potential and compared the changes in action potential duration to those observed during the after-potential. In seven preparations

a stable puncture was maintained during a total of fourteen exchanges of the perfusate in the single sucrose gap voltage clamp apparatus. The K concentrations of the test solutions were 1.5, 3, and 6 mM and the measurements were made 5–10 min after changes of solution. The resting potential was 82 ± 3 mV (s.d.). In a solution with 6 mM- K^+ the preparation depolarized 13.5 ± 1.5 mV (s.d.), and a solution with 1.5 mM- K^+ caused a hyperpolarization of 12 ± 1 mV (s.d.). The duration of the action potential was 550 ± 100 msec (s.d.) in a Ringer solution with 3 mM- K^+ . Increasing the K^+ content to 6 mM caused a $32 \pm 16\%$ (s.d.) shortening, and decreasing the K^+ content to 1.5 mM resulted in a $16 \pm 6\%$ (s.d.) prolongation of the action potential.

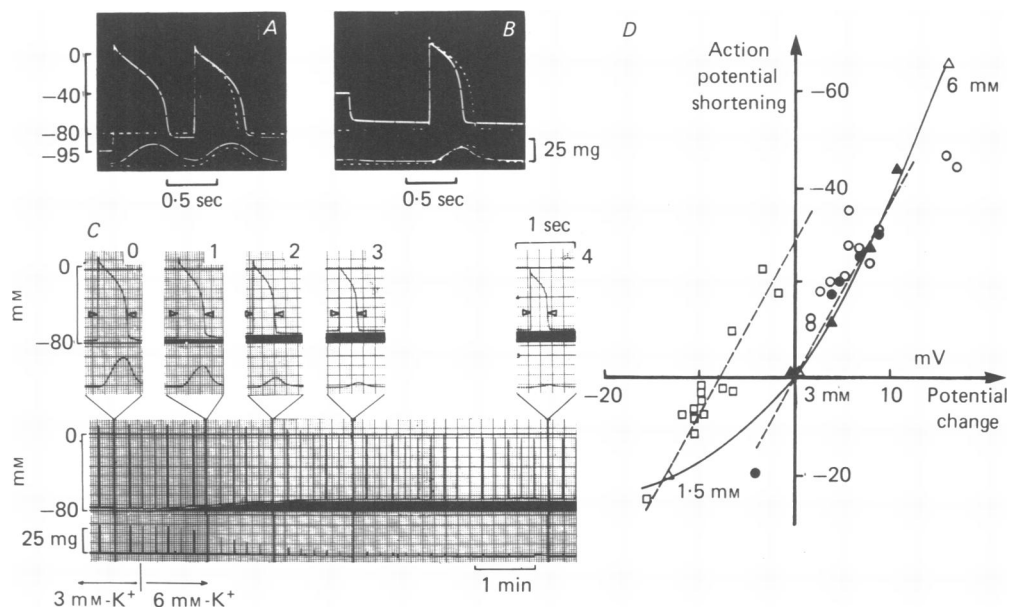


Fig. 14. Changes in membrane potential and action potential duration caused by voltage clamp induced K accumulation and by changes of the K concentration of the perfusate, K_o . The experiment illustrated in panels *A*, *B*, and *C* is represented by filled symbols in panel *D*. The changes in the membrane potential and the percentage change in the action potential are measured relative to the resting potential and the normal action potential recorded with $K_o = 3$ mM (dashed curves in panels *A* and *B*). Filled circles correspond to post clamp K accumulation (panels *A* and *B*) and filled triangles are recorded while K_o was increased from 3 to 6 mM (panel *C*). The open symbols in panel *D* correspond to another experiment. In this experiment K_o was altered in the sequence 3–6–3–1.5–3 mM (open triangles) and the effect of post-clamp K accumulation was studied with $K_o = 3$ mM (open circles) and $K_o = 1.5$ mM (open squares).

These observations indicate that the resting potential of the different preparations responds more consistently to variations in the extracellular K concentration than does the action potential duration. The change in the resting potential caused by variations in the extracellular K concentration can be described by eqn. (1.8) if K'_o is 1–1.5 mM.

Fig. 14 compares the relation between changes in membrane potential and action potential duration as obtained by post-clamp measurements (panels *A* and *B*) and by direct changes of $[K]_o$ (panel *C*). Panels *A* and *B* show action potentials following

a hyperpolarizing and a depolarizing clamp pulse, respectively. Filled circles on the graph (panel *D*) indicate values of membrane depolarization and action potential shortening obtained in this way. Filled triangles in panel *D* show the change in the shape of the action potential caused by an increase in $[K]_o$ from 3 to 6 mM. The results from another preparation which was subjected to voltage clamp pulses in 1.5 (open squares) and 3.0 mM- K^+ (open circles) are also plotted in panel *E*. The data points obtained from post-clamp measurements can be approximated by a straight line corresponding to 100% reduction in action potential duration for 30 mV depolarizing after-potential. Although the results suggest that fairly direct relations exist between the resting potential and the action potential duration both during post-clamp accumulation and during variations of $[K]_o$, the change in action potential duration produced by changes in $[K]_o$ were consistently smaller than the changes in action potential duration caused by comparable post-clamp depolarizations.

DISCUSSION

Evidence for extracellular K accumulation. Three parameters have been used as indicators of extracellular K accumulation: the after-potential, the action potential shortening and the K-electrode response. Results obtained using the three methods are in mutual agreement regarding some of the key observations supporting extracellular K accumulation. All three parameters consistently give N-shaped relations when plotted versus the clamped membrane potential. The maxima and the minima of this relation coincide with the maximum and minimum of the current-voltage relation measured at the end of 3–10 sec clamp pulses (Figs. 3 and 5). Thus, all three methods indicate that extracellular K accumulation occurs during long clamp pulses and that a major part of the maintained membrane current is carried by K ions. A rough calculation shows that the estimated magnitude of K accumulation agrees well with the magnitude of the measured membrane current. The decay of the post-clamp after-potential follows the same time course as the recovery of the normal action potential duration, suggesting that they are both closely related to changes in the extracellular K concentration (Fig. 13).

Further evidence for extracellular K accumulation is supplied by the experiments which show that the K accumulation calculated from the after-potential, unlike the after-potential itself, decays with a fairly well defined time constant as predicted by ionic diffusion (Fig. 11).

The linear equivalent circuit. Extracellular K^+ accumulation in the vicinity of the resting potential was described using a linear RC circuit. In this model K^+ accumulation occurs in a single compartment with one relaxation time. The model predicts that ionic accumulation can cause time dependent changes in the membrane current even in the absence of alteration in permeabilities. A similar model was introduced by Barry & Adrian (1973) to approximate the K^+ depletion in the T-tubules of frog skeletal muscle. As pointed out by these authors the accumulation of K^+ is caused by different transport numbers in various parts of the system.

Experiments illustrated in Figs. 8, 9, and 10 confirm the prediction of the model in the vicinity of resting potential by showing that (1) the initial membrane current is larger than the steady state current; (2) the time constant for the decay of after-

potential is larger than the time constant for decay of measured membrane currents; and (3) that the time course of decay of after-potential can be approximated by a single time constant. The model also provides a tool by which K⁺ accumulation in various preparations may be compared. Such a comparison showed remarkable consistency in accumulation processes from preparation to preparation. Some of the variations in the estimated values of the circuit elements in Table 1 could be related to changes in the size of the preparation.

Size and location of K⁺ accumulation space. Morphological studies on the frog ventricular muscle suggest that the extracellular space may be subdivided into the inter- and intratrabecular fractions (Page & Niedergerke, 1972). It is reasonable to assume that K⁺ would accumulate initially in the 9% intratrabecular fraction (subendothelial space) before diffusing through the endothelial sheath into the larger intertrabecular space of about 16%. Thus, it is the diffusion barrier between the two fractions of the extracellular space that determines to what extent K⁺ accumulation is distributed between the two spaces. The fractional value of these spaces is based on total extracellular space of 25% (Keenan & Niedergerke, 1967) and intratrabecular space of 10.4% of trabecular volume (Page & Niedergerke, 1972).

The experiments presented in this study make it possible to obtain an independent estimate of the volume of the accumulation space (V_e) using eqn. (1.20).

$$V_e = C_e \frac{RT}{F_2} \cdot \frac{1}{K_o + K'_o} \cdot \frac{G_{mK}}{G_{mK} + G_{mr}} \quad (1.20)$$

The accumulation capacity, C_e , was determined for a number of preparations from linear analysis and was found to be on average 260 μC (see Table 1). K_o is 3 mM and K'_o (an index for K⁺ selectivity of the membrane) is 1–1.5 mM. $G_{mK} + G_{mr}$, the total membrane conductance, is 222 μmhos ($1/R_m$, Table 1). The residual conductance, G_{mr} , was estimated from the membrane current measured in the minimum region (–20 mV) of the I – V relation. In this membrane potential range ΔV is small or absent (Figs. 3, 5 and 6) and it may be assumed that the measured membrane current (1–1.5 μA) is not carried by K⁺. (For a detailed discussion of the ionic nature of residual current, see Cleemann & Morad, 1978.) Thus this membrane current may provide an estimate of residual current. A linear residual current in the entire potential range (–80 to –20 mV) corresponds to a residual conductance (G_{mK}) of approximately 17–25 μmhos . The volume of K-accumulation space calculated from eqn. (1.20) using these values is from 1.35×10^{-8} to 1.59×10^{-8} l. The total volume of the preparation is approximately 10^{-7} l., calculated from the dimension of the preparation or from the membrane capacitance of the preparation (Goldman & Morad, 1977b). Based on these estimates, K⁺ must accumulate in a space corresponding to 13–16% of the preparation. These values should be considered as the upper estimate for the K⁺ accumulation space, since they are based on estimates of C_e which in turn is calculated from the magnitude of measured currents without correction for transgap leakage current (Goldman & Morad, 1977a). It is therefore apparent that the K⁺ accumulation space is significantly smaller than the total extracellular space and that accumulation may primarily occur in the subendothelial space (cf. Kline & Morad, 1978).

Redistribution of accumulated K⁺. If K⁺ primarily accumulates in the subendo-

thelial fraction of extracellular space, it may then be expected that diffusion of K^+ through the endothelial sheath plays a major role in the redistribution process. The time constant for redistribution of accumulated K^+ measured from the decay of the after-potential is 2.6 sec (see Table 1). This value may be compared to the 3–10 sec half-time of onset of Ca^{2+} inotropic action in superfused frog ventricular muscle (Chapman & Niedergérke, 1970). Morphological studies have shown that this delay may be related to the diffusion of Ca^{2+} through the narrow clefts of the endothelial sheath (Page & Niedergérke, 1972). If K^+ encounters similar diffusion barrier a time constant of 1.74–5.3 msec may be expected for more rapidly diffusing K^+ . Since the averaged measured value from our studies falls within this range it is likely that the endothelial sheath plays a primary role in redistribution of accumulated K^+ .

During the longer clamp pulses it is likely that some K will also accumulate in the larger intertrabecular fraction of the extracellular space thus producing two time constants for decay of accumulated K (Fig. 12). This assumption is consistent with the observation that K -selective micro-electrode measures a larger K accumulation in the centre of preparation than in the periphery during a period of rapid stimulation, and that thicker strips produced larger accumulation than thinner preparations (Kline & Morad, 1976, 1978).

Characteristic time constant for ionic diffusion in a cylindrical strip may be calculated (Crank, 1956) using ionic diffusion constant, the tortuosity factor (1.5, Page & Bernstein, 1964) and the diameter of the strip. Such calculation produces time constants on the same order as seen with long clamp pulses and measured by Kline & Morad (1978) following periods of rapid stimulation, using K^+ -selective electrodes. In the present study the typical clamp duration is considerably shorter than the commonly used intervals with rapid stimulation. It is, therefore, not surprising that the slow phase of the decay of the after-potential plays a less prominent role.

Which method gives the most accurate estimation of the extracellular K accumulation? A detailed comparison of the after-potential, the action potential shortening and the K electrode response indicates small systematic differences. Comparison of the post-clamp after-potential and the K electrode response indicates that the two parameters are not strictly proportional. Differences in the time course of decay have also been noted in a number of cases. Such differences may be in part due to the delay of K electrode response caused by withdrawal of the resin from the tip of the micropipette. Yet another reason for the discrepancy between the two methods may be due to the fact that K electrode measures the K activity at one location only while the after-potential probably is related to the average K^+ concentration in the immediate vicinity of the membrane.

Comparison of the effect of K on resting and action potential duration suggests that although there is a consistent relation between changes in resting potential and $[K]_o$ from preparation to preparation, there is considerable variation in changes in duration of action potential. It should also be noted that while the action potential is highly sensitive to ionic, drug, and temperature variations, the resting potential is fairly insensitive to experimental interventions other than changes in $[K]_o$. Therefore, the after-potential could serve as an ideal indicator of extracellular K^+ accumulation, if the membrane were perfectly K selective. However, it has been

previously shown (Brady & Woodbury, 1960; Harris & Morad, 1971) and confirmed in this study, for concentration range between 1.5 and 6 mM, that the membrane potential changes less than predicted by the Nernst equation. The experimental results could be approximated by the constant field equation (Goldman, 1943; Hodgkin & Katz, 1949) if it were assumed that the external Na and internal Cl carry an inward current equal to that carried by 1–1.5 mM of extracellular K ($K'_0 = 1\text{--}1.5$ mM). These results suggest that the K^+ selectivity of the membrane is sufficiently high as to make the after-potential a reliable tool in estimating the extracellular K^+ activity.

K^+ accumulation versus time dependent conductance changes. Considerable controversy exists as to whether slow current changes in skeletal and cardiac muscle are caused by time and voltage dependent permeability changes or extracellular K^+ accumulation (skeletal muscle: Adrian & Freygang, 1962; Adrian, Chandler & Hodgkin, 1970; Almers, 1972*a, b*; Barry & Adrian, 1973; in Cardiac Muscle: McAllister & Noble, 1966; McGuigan, 1974; Noble, 1976; Baumgarten & Isenberg, 1977). In order to use the after-potential as an effective indication of K activity in the extracellular space, it must be determined to what extent such permeability changes alter the ionic selectivity of the resting membrane. Around the resting potential, the linear analysis (Figs. 8, 9, 10) and the K^+ electrode measurements (Figs. 4, 5) show that both the after-potential and the slow current changes are directly related to K concentration changes. Around the resting potential therefore, slow time and voltage dependent permeabilities are small or absent. At more depolarizing potentials (-60 to $+30$ mV) there also exists a fairly good correlation between the magnitude of the after-potential and the K^+ electrode response. However, the correlation is not sufficiently close as to exclude completely that the time dependent permeability changes have an effect on the magnitude and time course of the after-potential. Further information regarding this point is derived from experiments where the decay of the after-potential was analysed in detail (Figs. 11, 12). Such analysis shows that the time course of the redistribution of accumulated K^+ is independent of the clamped membrane potential. This finding implies that 'true' time dependent permeability changes have negligible effect on the after-potential.

Inward-going K rectification. Both the membrane current measured at the end of the clamp pulse and the three indicators for extracellular K accumulation give N-shaped relations when plotted versus the clamped membrane potential. This suggests that the N-shaped current-voltage relations reflect primarily the voltage dependency of the K current and that the major fraction of the 'steady state' membrane current is carried by K. The minimum region in the current-voltage relations might be ascribed to inward current components carried by Na or Ca. In the light of the present investigation this is extremely unlikely. The accumulation studies support a strong inward-going rectification up to -20 mV. In the potential region from -40 to -20 mV the magnitude of the K accumulation even decreases thereby indicating that the K current falls. The properties of the inward-rectifying K current, which display this region of negative slope conductance, are described in detail in the following paper.

It would be of interest to know if post clamp hyperpolarizations around -20 mV really correspond to depletion of K^+ . The rate of active intracellular K uptake can

proceed at least at a rate of 0.05 m-mole/sec (Figs. 1 and 4, Gadsby, Niedergerke & Page, 1971). Therefore, the rate of K depletion in the extracellular space (approximately 5 times smaller than the intracellular compartment) may be as much as $0.05 \text{ m-mole/sec} \times 5 = 0.25 \text{ m-mole/sec}$. This number is of the same order of magnitude as that seen from direct measurement of depletion of K^+ using K electrodes (Martin & Morad, 1978). The corresponding hyperpolarization calculated from eqn. (1.8) for such an uptake rate is $RT/F \cdot ((3+1)/(3-0.25+1)) = 1.54 \text{ mV/sec}$. The largest measured hyperpolarizations for a clamp pulse of 3.5 sec is approximately 3 mV (see Fig. 6). It is therefore possible that the hyperpolarizing after-potential around -20 mV is caused by an active K reabsorption which is significantly larger than the passive K loss at the same potential.

We acknowledge the help of Dr R. P. Kline in providing us with potassium-selective electrodes. This work was supported by N.I.H. grant HL 16152.

REFERENCES

- ADELMAN, W. J., JR. & FITZHUGH, R. (1975). Solution of the Hodgkin-Huxley equations modified for potassium accumulation in a periaxonal space. *Fedn Proc.* **34**, 1322-1329.
- ADELMAN, W. J., JR., PALT, Y. & SENFT, J. P. (1973). Potassium ion accumulation in a periaxonal space and its effect on the measurement of membrane potassium ion conductance. *J. Membrane Biol.* **13**, 387-410.
- ADRIAN, R. H., CHANDLER, W. K. & HODGKIN, A. L. (1970). Slow changes in potassium permeability in skeletal muscle. *J. Physiol.* **208**, 645-668.
- ADRIAN, R. H. & FREYGANG, W. H. (1962). The potassium and chloride conductance of frog muscle membrane. *J. Physiol.* **163**, 61-103.
- ALMERS, W. (1972a). Potassium conductance changes in skeletal muscle and the potassium concentration in the transverse tubules. *J. Physiol.* **225**, 33-56.
- ALMERS, W. (1972b). The decline of potassium permeability during extreme hyperpolarization in frog skeletal muscle. *J. Physiol.* **225**, 57-83.
- BARRY, P. H. & ADRIAN, R. H. (1973). Slow conductance changes due to potassium depletion in the transverse tubules of frog muscle fibers during hyperpolarizing pulses. *J. Membrane Biol.* **14**, 243-292.
- BAUMGARTEN, C. M. & ISENBERG, G. (1977). Depletion and accumulation of potassium in the extracellular clefts of cardiac purkinje fibers during voltage clamp hyperpolarization and depolarization. *Pflügers Arch.* **368**, 19-31.
- BRADY, A. J. & WOODBURY, J. W. (1960). The sodium-potassium hypothesis as the basis of electrical activity in frog ventricle. *J. Physiol.* **154**, 385-407.
- CHAPMAN, R. A. & NIEDERGERKE, R. (1970). Effects of calcium on the contraction of the hypodynamic frog heart. *J. Physiol.* **211**, 389-421.
- CLEEMANN, L. & MORAD, M. (1976). Extracellular potassium accumulation and inward-going potassium rectification in voltage clamped ventricular muscle. *Science, N.Y.* **191**, 90-92.
- CLEEMANN, L. & MORAD, M. (1978). Potassium currents in frog ventricular muscle: evidence from voltage clamp currents and extracellular K accumulation. *J. Physiol.* **286**, 113-143.
- CRANK, J. (1956). *Mathematics of Diffusion*. London: Oxford University Press.
- FRANKENHAEUSER, B. & HODGKIN, A. L. (1956). The after-effects of impulses in the giant nerve fibres of *Loligo*. *J. Physiol.* **131**, 341-376.
- GADSBY, D. C., NIEDERGERKE, R. & PAGE, S. (1971). Do intracellular concentrations of potassium or sodium regulate the strength of the heart beat? *Nature, Lond.* **232**, 651-652.
- GOLDMAN, D. E. (1943). Potential, impedance, and rectification in membranes. *J. gen. Physiol.* **27**, 37-60.
- GOLDMAN, Y. & MORAD, M. (1977a). Measurement of transmembrane potential and current in cardiac muscle: A new voltage clamp method. *J. Physiol.* **268**, 613-654.
- GOLDMAN, Y. & MORAD, M. (1977b). Ionic membrane conductance during the time course of the cardiac action potential. *J. Physiol.* **268**, 655-695.

- HARRIS, J. E. & MORAD, M. (1971). The effect of Ca-K interaction on the plateau of the cardiac action potential. *The Physiologist* **14**, 159.
- HODGKIN, A. L. & KATZ, B. (1949). The effect of sodium ions on the electrical activity of the giant axon of the squid. *J. Physiol.* **108**, 37-77.
- KEENAN, M. J. & NIEDERGERKE, R. (1967). Intracellular sodium concentration and resting sodium fluxes of the frog heart ventricle. *J. Physiol.* **188**, 235-260.
- KLINE, R. & MORAD, M. (1976). Potassium efflux and accumulation in heart muscle: Evidence from K⁺-electrode experiments. *Biophys. J.* **16**, 367-372.
- KLINE, R. P. & MORAD, M. (1978). K⁺ efflux in heart muscle during activity: Extracellular accumulation and its implications. *J. Physiol.* **280**, 537-558.
- LAMB, J. F. & MCGUIGAN, J. A. S. (1968). The efflux of potassium, sodium, chloride, calcium and sulphate ions and of sorbitol and glycerol during the cardiac cycle in frog's ventricle. *J. Physiol.* **195**, 283-315.
- MCALLISTER, R. E. & NOBLE, D. (1966). The time and voltage dependence of the slow outward current in cardiac Purkinje fibres. *J. Physiol.* **186**, 632-662.
- MCGUIGAN, J. A. S. (1974). Some limitations of the double sucrose gap, and its use in a study of the slow outward current in mammalian ventricular muscle. *J. Physiol.* **240**, 775-806.
- MARTIN, G. & MORAD, M. (1978). K⁺ efflux and uptake in frog ventricular muscle. *Biophys. J.* **21**, 166a.
- MORAD, M. & ORKAND, R. K. (1971). Excitation-contraction coupling in frog ventricle: evidence from voltage clamp studies. *J. Physiol.* **219**, 167-189.
- NEHER, E. & LUX, H. D. (1973). Rapid changes of potassium concentration at the outer surface of exposed single neurons during membrane current flow. *J. gen. Physiol.* **61**, 385-399.
- NIEDERGERKE, R. & ORKAND, R. K. (1966). The dual effect of calcium on the action potential of the frog's heart. *J. Physiol.* **184**, 291-311.
- NOBLE, S. J. (1976). Potassium accumulation and depletion in frog atrial muscle. *J. Physiol.* **258**, 579-613.
- PAGE, E. & BERNSTEIN, R. S. (1964). Cat heart muscle *in vitro*: Diffusion through a sheet of right ventricle. *J. gen. Physiol.* **47**, 1129-1140.
- PAGE, S. G. & NIEDERGERKE, R. (1972). Structures of physiological interest in the frog heart ventricle. *J. cell Sci.* **11**, 179-203.
- WALKER, J. L. (1971). Ion specific liquid ion exchanger microelectrodes. *Analyt. Chem.* **43**, 89A-93A.